Simplified Design of Axial-Flow Cyclone Mist Eliminators

E. Brunazzi and A. Paglianti
Laboratory of Process Equipment, Dept. of Chemical Engineering, Industrial Chemistry and Materials Science

A. Talamelli
Dept. of Aerospace Engineering
University of Pisa, I-56126 Pisa, Italy

Mist eliminators have widespread application in many processes, and a large number of different types of mist eliminators are available on the market. Wire-mesh mist eliminators, vane-type eliminators, and cyclones are used extensively in many industrial plants. Unfortunately, these separators present some significant drawbacks when they are used in high-pressure applications or in any application in which a reduction in the diameter of the vessel containing the separator is necessary and high separation efficiency is required. Therefore, over the last several years some important suppliers have developed new axial flow separators (such as Axiflow, Swirl Tube, or Vico-Spin). Despite the broad range of entrainment removal applications, open literature on this topic is scarce. So far, design of these axial-flow separators can only be performed by suppliers using proprietary design criteria or using semiempirical equations with an uncertain range of applicability. This work presents new experimental data obtained at atmospheric conditions on three different axial separators and a new design model.

Introduction

Entrained liquid may be required to be removed from gas or vapor streams for many reasons in industrial plants, for example, to recover valuable products dispersed in the process stream, to increase the vapor- or gas-stream purity, to protect downstream equipment from corrosive liquids, or to improve emission controls. Selection of the proper collection equipment depends mainly on the size distribution of the entrained liquid droplets and has been the subject of many articles (Holmes and Chen, 1984; Fabian et al., 1993; Svrcek and Monnery, 1993; Capps, 1994; Ziebold, 2000). Unfortunately, most of the works published so far for the selection neglect the existence of axial flow cyclones. This absence may have been acceptable up until a few years ago, but nowadays this is no longer the case. Due to the development of new axial flow separators and their increasing presence on the market, design criteria for these new types of separator are needed.

Axial flow separators impart a very high centrifugal force on the entering gas stream. This allows a high separation efficiency and increased handling capacity, which permits a reduction in the vessel diameter compared to that for vane-type or wire-mesh mist eliminators.

The maximum superficial gas velocity through a mist eliminator, and, therefore, the vessel diameter, has usually been evaluated using the Souders–Brown relation

$$u_{sg,\max} = K \cdot \sqrt{\frac{\rho_l - \rho_g}{\rho_g}} \tag{1}$$

where $u_{sg,\max}$ is the maximum superficial gas velocity and ρ_l and ρ_g are, respectively, the density of the liquid and gas phases. The K values have to be experimentally determined because they depend on the physical properties of the working fluids, on the deentrainment height, and somewhat on the system pressure (Ludwig, 1995). For vertical flow in vane-type and wire-mesh mist eliminators, Holmes and Chen (1984) and York and Poppele (1963) give an average design K-factor of 0.35 ft/s (0.11 m/s). Use of Eq. 1 permits evaluation of the superficial gas velocity, and, therefore, the vessel dimension of a separator equipped with either a vane-type or

Correspondence concerning this article should be addressed to A. Paglianti.

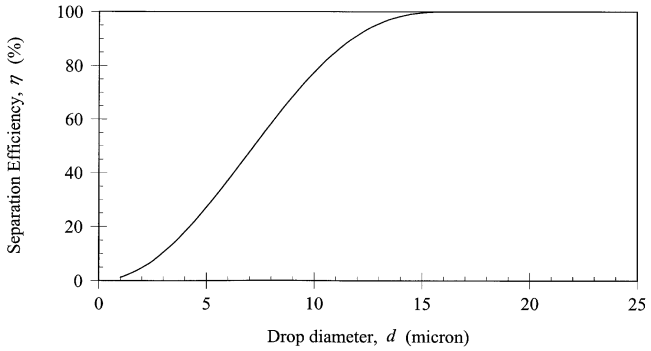

Figure 1. Separation efficiency vs. drop diameter.

Theoretical trend according to Brunazzi and Paglianti (1998). Packing characteristics: 270 m^2/m^3, wire diameter 270 μm, pad thickness 150 mm. Working conditions: air–water system, pressure 7 MPa, temperature 20°C, superficial gas velocity 0.37 m/s.

a wire-mesh mist eliminator. If, for instance, we assume that mist has to be removed from 100,000 kg/h of air at 7 MPa and 20°C, Eq. 1 suggests that the maximum allowable gas velocity is about 0.37 m/s, which implies that a vessel diameter of 1070 mm is needed. It is important to point out that this vessel diameter is the minimum diameter because, as shown by Ludwig (1995), the *K*-factor slowly decreases with increasing working pressure. In this case, if a wire-mesh mist eliminator is used, it is possible to predict separation performance using the model by Brunazzi and Paglianti (1998). Figure 1 shows the separation efficiency that can be obtained with a commonly used wire-mesh mist eliminator with a specific surface area of 270 m^2/m^3 and a wire diameter of 270 microns. Figure 1 also shows that the value of dp_{100}, which is the smallest droplet diameter that can be separated with a 100% efficiency, is about 20 microns.

The low separation efficiency in the 5–10 micron range of drop diameter and the large vessel diameter required to contain the wire-mesh mist eliminator both explain why some new separators have been designed especially for high gas density applications in the last few years. In addition, the new separators are easily cleaned, they continue operating even if some solids are present in the inlet flow, and they are easily inserted through manholes.

The present work examines three different types of axial flow separators experimentally at atmospheric working conditions. The experimental investigation considered droplet size from around 1 micron upwards, particular attention being focused on the overlapping size region between the coarsest mist particles and the finest spray particles. A model for the collection performance of the tested axial flow cyclones has been developed, using a number of simplifying assumptions. Two different approaches concerning droplet behavior in the axial flow separator have been considered. For the one based on the complete radial mixing concept, it is assumed that, because of the turbulent mixing, the concentration of uncollected droplet is uniform across any horizontal cross section of the separator and that removal occurs across a thin layer at the outer wall. For the other approach, which is based on the absence of a radial mixing concept, it is assumed that droplets behave as if they are in a laminar flow and move as a plug toward the outer wall. The results of the model using either the former or the latter approach are compared with the experimental data.

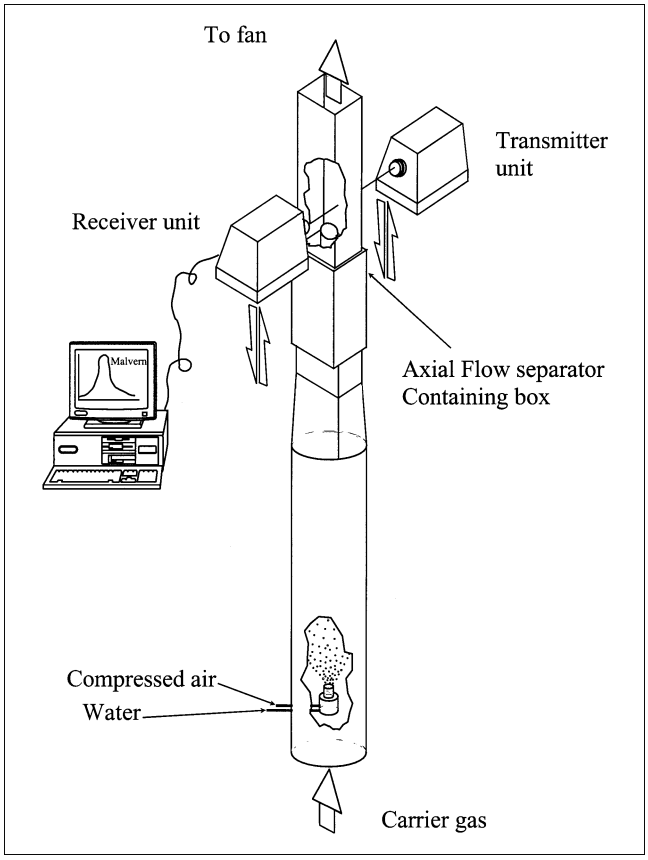

Figure 2. Experimental test apparatus.

Experimental Loop

Experimental collection efficiencies were determined as a function of droplet size and gas velocity at atmospheric working conditions in an experimental loop designed and built at the Chemical Engineering Department of the University of Pisa. For this purpose, different types of axial flow mist eliminators, furnished by Costacurta S.p.A. VICO, were tested. Air and water were used as working fluids. The experimental rig mainly consisted of a spray-generation circuit and an air-carrier circuit. The spray was generated using an ultrasonic nozzle fed by a volumetric pump, giving liquid flow rates of between 0 and 2,600 L/h, and by a compressor supplying air at 0.6 MPa at flow rates of up to 280 m^3/h at standard conditions.

The test section, shown in Figure 2, consisted of a 3-m-long metal measuring section with a rectangular cross section, 120 mm wide and 190 mm high. The separator was installed vertically with respect to the upflow of gas. A Malvern Particle Sizer instrument, based on measurements of the diffraction of a He–Ne laser beam of droplets moving through the measuring section, was used to accurately measure the total droplet concentration and volumetric droplet distribution (Brunazzi and Paglianti, 1998, 2000). Acquisitions were carried out both upstream and downstream of the separator.

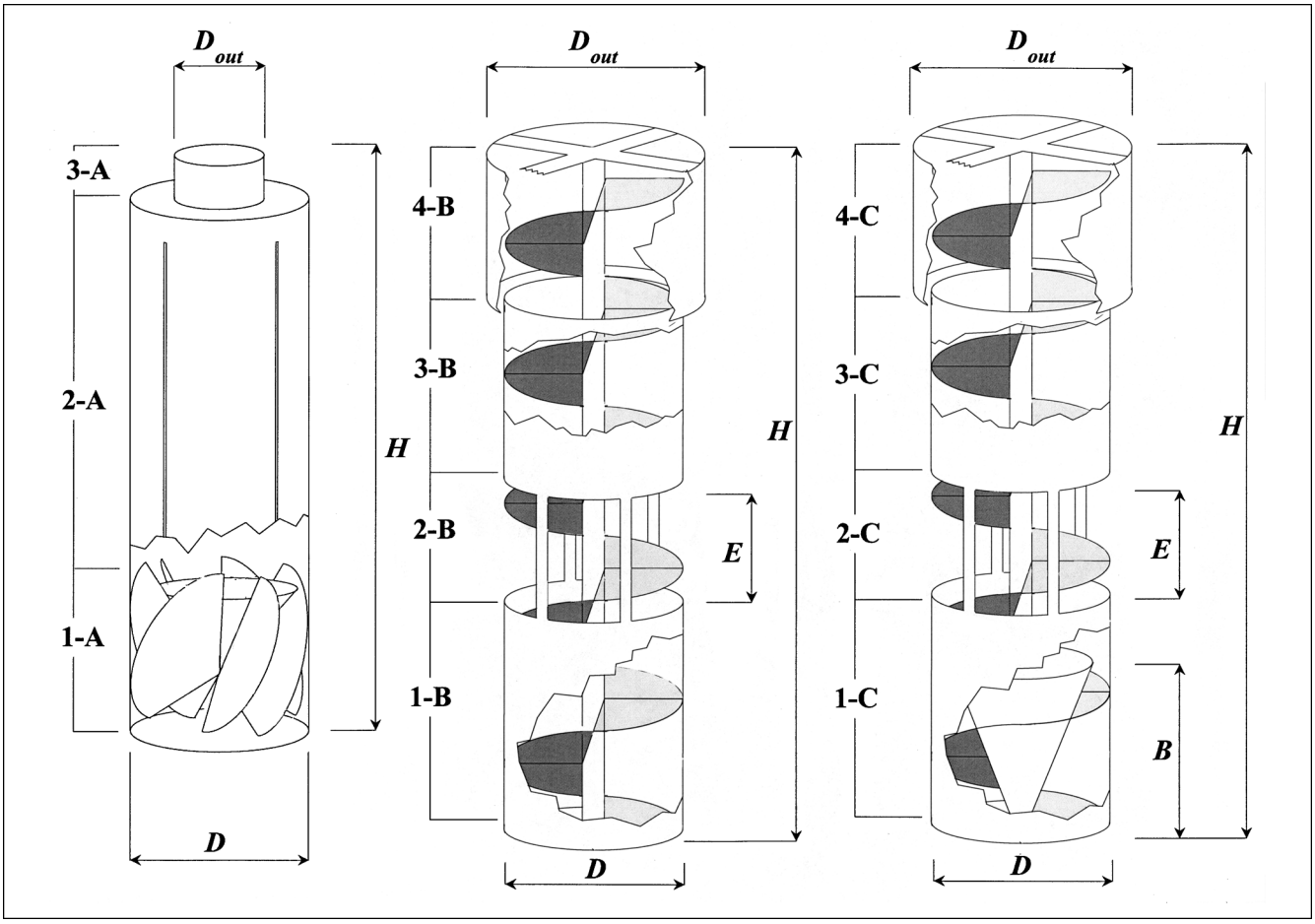

Figure 3. Tested cyclones.

Each data point represents the average of six different acquisitions. The accuracy of the measured efficiency is quite high and the maximum uncertainty of the measured efficiency is below 5%.

This article analyzes three axial flow separators, plotted in Figure 3, whose main geometrical characteristics are shown in Table 1. The axial separator shown in Figure 3A is formed by a swirler 170 mm in length made up of six flat deflected vanes. This swirler is located inside a tube that has an inner diameter of 110 mm and is 500 mm long; the collected liquid is drained off into a separate external concentric tube through four 4-mm-wide vertical slits. The axial flow separator shown in Figure 3B is formed from a continuous single-threaded helix 670 mm in length located inside a tube with an inner diameter of 135 mm. The drainage system is formed from a 100-mm-long vent that allows the separated liquid to drain into an external concentric tube. The top of the separator shows an external concentric tube around the helix, with an inner diameter of 210 mm, that has the goal of increasing the gas-velocity limit before reentrainment occurs. The axial flow separator shown in Figure 3C is quite similar to that shown in Figure 3B; the helix is single-threaded and the only difference is the presence of the 230-mm-long filled cone at the bottom.

Model to Simulate Axial Flow Separator

The gas flow in axial cyclones is intrinsically three-dimensional and turbulent. Unfortunately, even though in the last few years the computational fluid dynamic (CFD) approach has made important progress, so far it can only be used to obtain a proper evaluation of pressure drops across these

Table 1. Geometric Characteristics of the Cyclones

Type	Cyclone Dia. D (mm)	Cyclone Hgt. H (mm)	Discharge Hole Hgt., E (mm)	Vane Blade Vertical Angle (deg)	Outlet Dia. D_{out} (mm)	Total Rev. No.	Cone Hgt., B (mm)
3.A	110	500	—	30	54	1.8	—
3.B	135	670	100	70	210	6	—
3.C	135	670	100	70	210	6	230

separators, but cannot provide a good prediction of separation efficiency (Babbore, 2000). It is, therefore, necessary to develop simplified approaches based on the study of droplet trajectories. By using simple models for the particle mechanics and the gas flow through the cyclone, it is possible to calculate the particle trajectories and, hence, collection efficiencies. This simplified approach was applied by Licht (1980) for the study of common cyclones, with interesting results.

The present work presents an approach based on the study of droplet trajectories. In particular, depending on the description of droplets mixing on any horizontal cross section of the axial cyclone, the present approach leads to two different models. In fact, the mixing of droplets inside the gas–liquid separator is still an open question. One of two cases can be assumed: either (1) perfect mixing in any horizontal cross section of the separator, as has been considered by Carpenter and Othmer (1955) for wire-mesh separators and by Dietz (1981) for cyclones, among others , or (2) the absence of mixing, as considered by Brunazzi and Paglianti (1998) for wire-mesh separators, and by Verlaan (1991) for axial-flow cyclones. Therefore, the present work will analyze both perfect mixing and the absence of mixing hypotheses. This will lead to two different models that can take the different fluid dynamic behaviors into account.

Both models that will be presented are based on the following two hypotheses: (1) no reentrainment into the gas stream of already collected liquid, and (2) no buildup of liquid inside the separator.

The present models are based on the simplifying hypothesis that while the velocity vector of a liquid drop can have both tangential and radial components, as well as the axial one, the gas stream has only axial and tangential velocity components. In other words, it has been assumed that the radial component of the gas velocity vector, u_r, is nil in the whole separator. A droplet with a tangential velocity equal to, $v_{\theta,0}$, at time $t = 0$, flows in the separator as shown in Figure 4. Another widely used simplifying hypothesis is to neglect the tangential slip velocity between gas and droplets. Thus, the gas and the droplet tangential velocities are the same, that is, $u_\theta = v_\theta$.

As regards the gas flow through the cyclone, it has been assumed that the ratio between tangential and axial velocity depends only on the swirling element and does not change along the length of the separator. This simplifying hypothesis is strictly valid only for "short" cyclones. The present work analyzes only cyclones with length-to-diameter ratios below 5. Therefore, according to Bürkholz (1989), in this case the rotational moment decreases less than 10%. It is obvious that the present simplified analysis cannot be used for "long" cyclones, in which the decrease of angular momentum as a function of the tube length has to be taken into account.

Several earlier workers who studied common cyclones assumed that the gas flow constituted a form of vortex such that the tangential gas velocity is a function of the distance from the center and can be computed as

$$u_\theta \cdot r^n = C \tag{2}$$

where C is a constant, depending on the geometry of the equipment, and n depends on the geometry and on the working temperature. For ideal flow in a vortex, $n = 1$, whereas, for real flow, n can be computed using semiempirical equations. The present work uses the relation by Licht (1980), which is based on experimental data by Alexander (1980). This gives

$$n = 1 - \left[1 - 0.67 \cdot (2 \cdot r_2)^{0.14}\right] \cdot \left(\frac{T}{283}\right)^{0.5} \tag{3}$$

where T is the working temperature in degrees kelvin, and r_2 is the outer radius of the cyclone, in meters.

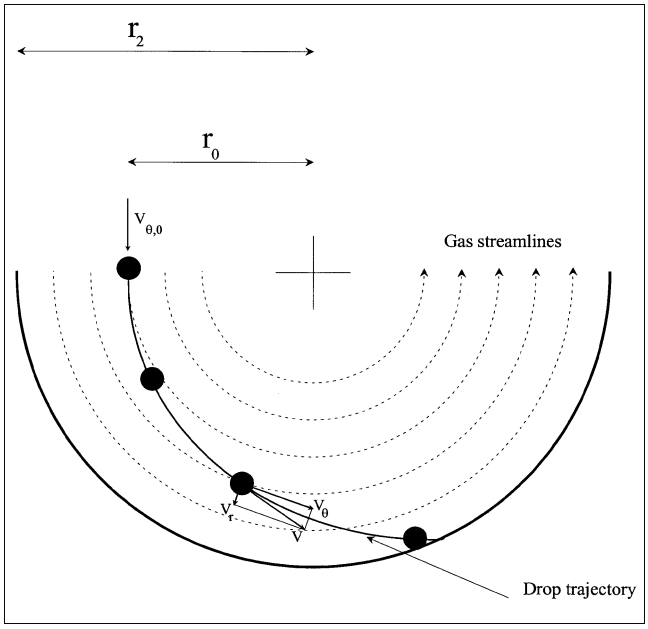

Figure 4. Drop trajectory.

As regards the flow of the liquid drops, the force balance in the radial direction on the single drop has been simplified by considering only the centrifugal force and the shear force. Assuming that the drop is spherical, the force balance assumes the following form

$$\rho_l \cdot \pi \cdot \frac{d^3}{6} \cdot \frac{dv_r}{dt} = (\rho_l - \rho_g) \cdot \pi \cdot \frac{d^3}{6} \cdot \frac{v_\theta^2}{r} - \frac{1}{2} \cdot C_D \cdot \rho_g \cdot v_r^2 \cdot \left(\frac{\pi \cdot d^2}{4}\right) \tag{4}$$

where $v_r = dr/dt$ and, due to the low value of the radial velocity, the drag coefficient, C_D, has been evaluated using the Stokes' law. Therefore, Eq. 4 can be rewritten as

$$\frac{d^2 r}{dt^2} = \frac{\rho_l - \rho_g}{\rho_l} \cdot \frac{u_\theta^2}{r} - 18 \cdot \frac{\mu_g}{\rho_l \cdot d^2} \cdot \left(\frac{dr}{dt}\right) \tag{5}$$

Nevertheless, if the Reynolds number is more than unity, the influence of the Reynolds number on the drag coefficient has to be taken into account.

A good approximation is achievable by neglecting the second-order terms in Eq. 5. This enables it to be simplified, which, together with the insertion of Eq. 2, results in the following

$$\frac{dr}{dt} = \frac{(\rho_l - \rho_g)\cdot d^2}{18\cdot\mu_g}\cdot\frac{u_{\theta,0}^2\cdot r_0^{2\cdot n}}{r^{2\cdot n+1}} \tag{6}$$

Integrating the previous equation from $t = 0$ to a generic instant in time, t, the following is derived

$$t = \frac{r_0^2}{2\cdot(n+1)\cdot u_{\theta,0}^2}\cdot\frac{18\cdot\mu_g}{d^2\cdot(\rho_l-\rho_g)}\cdot\left[\left(\frac{r}{r_0}\right)^{2\cdot(n+1)} - 1\right]$$

$$= \frac{r_2^2}{2\cdot(n+1)\cdot u_{\theta,2}^2}\cdot\frac{18\cdot\mu_g}{d^2\cdot(\rho_l-\rho_g)}$$

$$\cdot\left[\left(\frac{r}{r_2}\right)^{2\cdot(n+1)} - \left(\frac{r_0}{r_2}\right)^{2\cdot(n+1)}\right] \tag{7}$$

Figure 5A shows a generic horizontal cross section of a separator. In an infinitive time, dt, only the droplets whose distances from the wall are less than dr can be effectively collected. As previously anticipated, two different numerical approaches are now possible. The key difference between these concerns droplet behavior in the separator. We can either consider that, because of the turbulent flow field in the separator, the droplets in each sector of the cyclone are perfectly mixed along the radius, and, therefore, no concentration gradient of droplets exists in any horizontal cross section, or we can assume that no mixing occurs, and so the droplets behave as if they were in a laminar flow and move as a plug toward the wall. When the former approach is used, assumption is made that in a thin layer at the separator outer wall, where droplet removal occurs, droplet motion can be considered under laminar flow conditions and the Stokes' law is applicable. This assumption was applied with interesting results in the study of common cyclone separators (Flagan and Seinfeld, 1988).

Complete radial mixing

The assumption of complete radial mixing supposes that the droplets are well-mixed, due to turbulence and eddies in the gas stream; therefore, a uniform concentration of uncollected droplets is maintained in any horizontal cross section of the separator. Droplet removal occurs across a thin layer at the separator's outer wall. Plug flow is assumed along the axial direction. Under these hypotheses, the mass balance on a sector with thickness dz and angle $d\theta$ can be written as

$$-dN = \frac{d\theta}{2}\cdot\left[r_2^2 - (r_2 - dr)^2\right]\cdot dz\cdot X \tag{8}$$

where N is the total number of droplets in the control volume and X is the numerical droplet concentration. The total

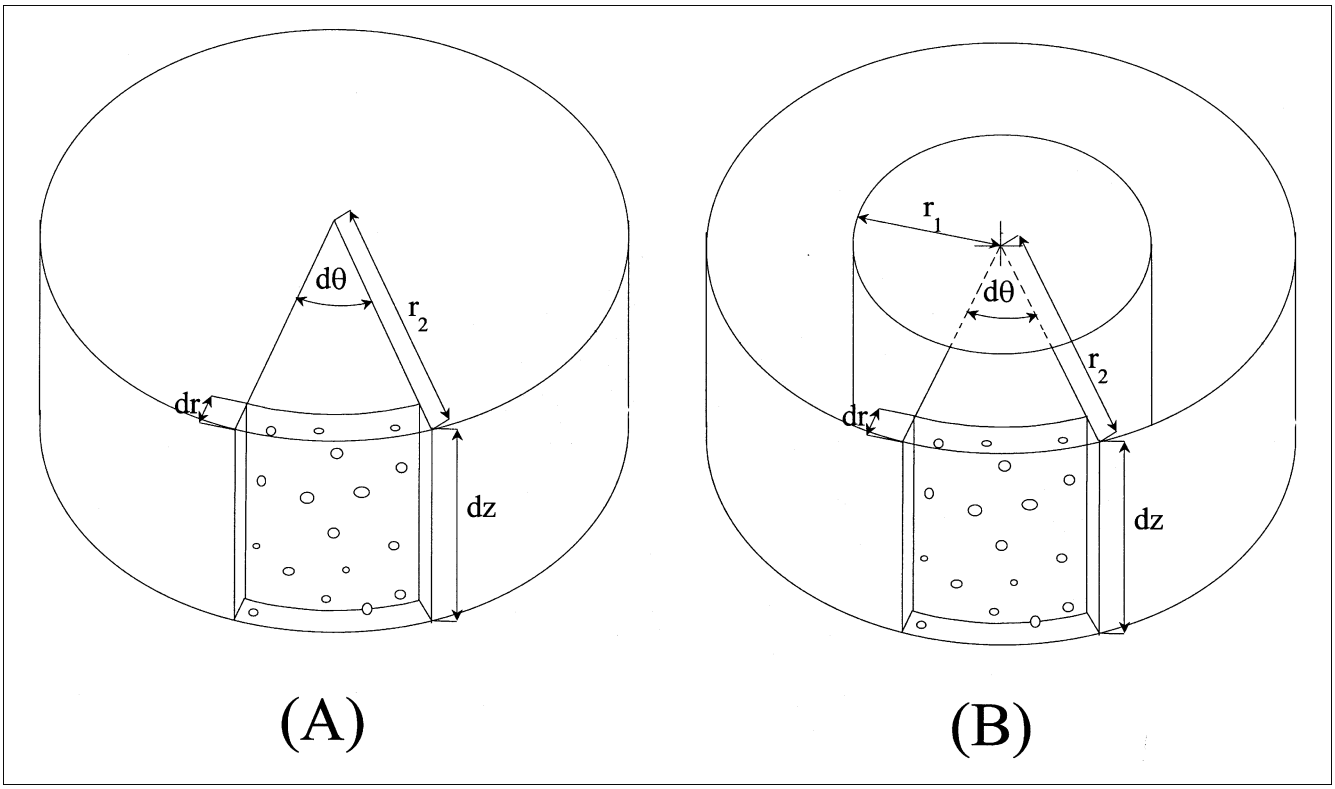

Figure 5. Cyclone cross section: (A) flow in the whole cross section; (B) flow in an annulus cross section.

number of droplets contained in the control volume is

$$N = X \cdot \frac{d\theta}{2} \cdot r_2^2 \cdot dz \tag{9}$$

and the fraction of captured droplets is

$$-\frac{dN}{N} = \frac{2 \cdot r_2 \cdot dr - dr^2}{r_2^2} \approx \frac{2 \cdot dr}{r_2} \tag{10}$$

Equation 7 gives the relationship between time and radial position of the single droplet. Therefore, introduction of Eq. 7 into Eq. 10 permits the fraction of collected droplets to be expressed as a function of time. In addition, under the hypothesis of complete mixing, each as yet uncollected droplet is remixed uniformly at each instant over the horizontal cross section of the cyclone, despite the fact that the total number of droplets decreases with increasing residence time. Thus, the mass center of the droplets not captured coincides with the vortex center at each instant t, and we can, therefore, assume that $r_0 = 0$ in Eq. 7. Thus, Eq. 10 can be rewritten as

$$\frac{dN}{N} = -2 \cdot \frac{d^2 \cdot (\rho_l - \rho_g)}{18 \cdot \mu_g} \cdot \frac{u_{\theta,2}^2}{r_2^2} \cdot \left[2 \cdot (n+1) \cdot \frac{d^2 \cdot (\rho_l - \rho_g)}{18 \cdot \mu_g} \cdot \left(\frac{u_{\theta,2}^2}{r_2^2} \right) \right]^{-(2 \cdot n + 1)/(2 \cdot n + 2)} \cdot t^{-(2 \cdot n + 1)/(2 \cdot n + 2)} \cdot dt \tag{11}$$

Finally, integration of Eq. 11 over a residence time, t_{res}, in the separator gives

$$\eta = 1 - \exp\left[-2 \cdot \left[2 \cdot (n+1) \cdot \frac{d^2 \cdot (\rho_l - \rho_g)}{18 \cdot \mu_g} \cdot \left(\frac{u_{\theta,2}^2}{r_2^2} \right) \cdot t_{res} \right]^{1/(2 \cdot n + 2)} \right] \tag{12}$$

Equation 12 can be used if the whole cross section of the axial flow cyclone is available for the two-phase flow, whereas, if the mixture flows in an annulus, as shown in Figure 5B, Eq. 9 assumes a different form

$$N = X \cdot \frac{d\theta}{2} \cdot \left(r_2^2 - r_1^2 \right) \cdot dz \tag{13}$$

and, therefore, Eqs. 11 and 12 assume the following form

$$\frac{dN}{N} = -2 \cdot \frac{d^2 \cdot (\rho_l - \rho_g)}{18 \cdot \mu_g} \cdot \frac{u_{\theta,2}^2}{\left(r_2^2 - r_1^2 \right)} \cdot \left[2 \cdot (n+1) \cdot \frac{d^2 \cdot (\rho_l - \rho_g)}{18 \cdot \mu_g} \cdot \left(\frac{u_{\theta,2}^2}{r_2^2} \right) \right]^{-(2 \cdot n + 1)/(2 \cdot n + 2)} \cdot t^{-(2 \cdot n + 1)/(2 \cdot n + 2)} \cdot dt \tag{14}$$

$$\eta = 1 - \exp\left[-\frac{2}{r_2^2 - r_1^2} \cdot \frac{1}{\left(r_2^2 \right)^{-(2 \cdot n + 1)/(2 \cdot n + 2)}} \cdot \left[2 \cdot (n+1) \cdot \frac{d^2 \cdot (\rho_l - \rho_g)}{18 \cdot \mu_g} \cdot u_{\theta,2}^2 \cdot t_{res} \right]^{1/(2 \cdot n + 2)} \right] \tag{15}$$

Absence of radial mixing

When using the absence of the droplet mixing approach, the present model assumes that all the droplets are uniformly distributed across the inlet cross section of the separator and that the trajectories of all droplets with the same size make up a family of parallel curves. Therefore, in the absence of mixing, the separation efficiency of the droplets with diameter, d, can be easily evaluated from the knowledge of position r' of the innermost particle that, after a time equal to the residence time, t_{res}, arrives at a radial position equal to the outer radius of the cyclone, r_2.

Analyzing the case of a separator whose geometrical characteristics are shown in Figure 5B, and by inserting Eq. 2 into Eq. 6, we get

$$\frac{dr}{dt} = \frac{d^2 \cdot (\rho_l - \rho_g)}{18 \cdot \mu_g} \cdot \frac{C^2}{r^{2 \cdot n + 1}} \tag{16}$$

Integrating, it is possible to evaluate r'

$$r' = \left[r_2^{2 \cdot (n+1)} - \frac{d^2 \cdot (\rho_l - \rho_g)}{18 \cdot \mu_g} \cdot C^2 \cdot t_{res} \cdot 2 \cdot (n+1) \right]^{1/(2 \cdot (n+1))} \tag{17}$$

and, therefore, the efficiency

$$\eta = \frac{r_2^2 - r'^2}{r_2^2 - r_1^2} \tag{18}$$

Equation 18 also allows the separation efficiency to be evaluated for a cyclone with geometrical characteristics shown in Figure 5A. In this case, it is sufficient to substitute $r_1 = 0$ in Eq. 18.

The flow field

Both in the case of perfect radial mixing and in the absence of mixing, in order to evaluate the separation efficiency, it is necessary to know the mean residence time, t_{res}, in the cyclone and the tangential velocity, $u_{\theta,2}$ at the wall of the cyclone or, equivalently, the value of the constant C. Strictly speaking, the value of $u_{\theta,2}$ is nil because of the presence of the boundary layer. Licht (1980) suggested using the average gas inlet velocity for a conventional cyclone; in the present work, a value of $u_{\theta,2}$ will be used, which will derive from the mass balance on the gas phase and from the use of Eq. 2.

The mass balance on the gas phase assumes the following

form

$$\bar{u}_\theta \cdot (r_2 - r_1) = \int_{r_1}^{r_2} u_\theta \cdot dr \tag{19}$$

where $\bar{u}_\theta$ is the mean value of the tangential gas velocity. Using Eq. 2 and integrating Eq. 19, we get

$$C = \bar{u}_\theta \cdot (1-n) \cdot \frac{(r_2 - r_1)}{r_2^{1-n} - r_1^{1-n}} \tag{20}$$

We need to know $\bar{u}_\theta$ to evaluate C. Thus, focusing attention on the tangential velocity, and assuming a constant value of the angular momentum along the cyclone length, it is possible to evaluate the mean residence time, t_θ, as

$$t_\theta = \frac{\pi \cdot \left(r_2^2 - r_1^2\right) \cdot \bar{N}}{\bar{u}_\theta \cdot (r_2 - r_1)} \tag{21}$$

where $\bar{N}$ is the number of revolutions inside the separator.

On the other hand, if we focus attention on the axial velocity, it is possible to evaluate the residence time, t_a, as

$$t_a = \frac{L}{Q} \cdot \pi \cdot \left(r_2^2 - r_1^2\right) \tag{22}$$

where Q is the gas volumetric flow rate and L is the separator length. By imposing the condition that the residence times computed using either the tangential or the axial velocities are identical, that is, $t_{\text{res}} = t_\theta = t_a$, we get

$$\bar{u}_\theta = Q \cdot \frac{\bar{N}}{L \cdot (r_2 - r_1)} \tag{23}$$

Therefore, knowledge of the geometrical characteristics of the cyclone and the gas volumetric flow rate allows us to compute the average tangential velocity and the residence time. These, in turn, allow us to evaluate C from Eq. 20, and finally to calculate $u_{\theta,2}$, which is required for evaluation of the separator efficiency.

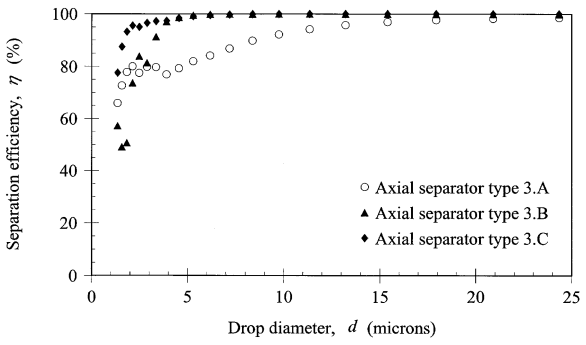

Figure 6. Separation efficiency of tested cyclones vs. drop diameter.

Working conditions: Air-water system, pressure 0.1 MPa, temperature 20°C, superficial gas velocity 5 m/s.

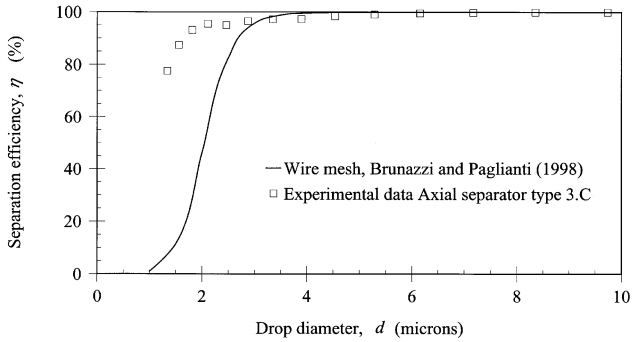

Figure 7. Separation efficiency vs. drop diameter.

Comparison between present experimental measurements on cyclone type 3.C and wire-mesh mist eliminator. Wire-mesh packing characteristics: 270 m^2/m^3, wire diameter 270 microns, pad thickness 150 mm. Working conditions: air–water system, pressure 0.1 MPa, temperature 20°C, superficial gas velocities of 3.18 m/s for wire-mesh mist eliminator (the maximum allowable according to Holmes and Chen, 1984), and 5 m/s for cyclone type 3.C.

Analysis of Experimental Results

It is now possible to analyze the experimental separation efficiency of the axial flow cyclones described in the previous paragraphs. Figure 6 shows the measured separation efficiencies of these axial flow cyclones as a function of droplet diameter; in all cases, the superficial velocity of the gas phase was 5 m/s. The figure shows that the axial cyclone labeled 3.A presents a dp_{100} value of about 15 microns, whereas the separators labeled 3.B and 3.C show dp_{100} values of about 5 microns. The figure also shows that the separator labeled 3.C performs somewhat better than the 3.B configuration. It is important to point out that all three types of cyclone show a good separation efficiency for droplet diameters in the range of 1–2 microns. This result is important when these experimental results are compared with the separation efficiency of common wire-mesh mist eliminators. Figure 7 shows the separation efficiency of cyclone 3.C, measured under a superficial gas velocity of 5 m/s, compared with the efficiency of a common wire-mesh pad, computed at 3.18 m/s, according to the model by Brunazzi and Paglianti (1998) [the maximum allowable gas phase superficial velocity at atmospheric conditions and with an air–water system, according to Holmes and Chen (1984)]. The specific surface of the wire-mesh mist eliminator is 270 m^2/m^3, the thickness is 150 mm, and the wire diameter is equal to 270 microns. The figure shows that axial flow separators permit the highest separation efficiency to be obtained even for small droplets. Moreover, it must be emphasized that, because of their geometrical characteristics, axial flow cyclones can also be used in the presence of solid particles, which is a field where the use of wire-mesh mist eliminators is not advisable.

It is now possible to compare the experimental data obtained in this work, with the computed values obtained using both of the models previously shown and also the semiempirical equation suggested by Bürkholz (1989). To our knowledge, the equation suggested by Bürkholz (1989) is the only one available so far in the open literature.

Cyclone type 3.A has been divided into three parts for computational reasons: 1-A, 2-A, 3-A (see Figure 3); the lower

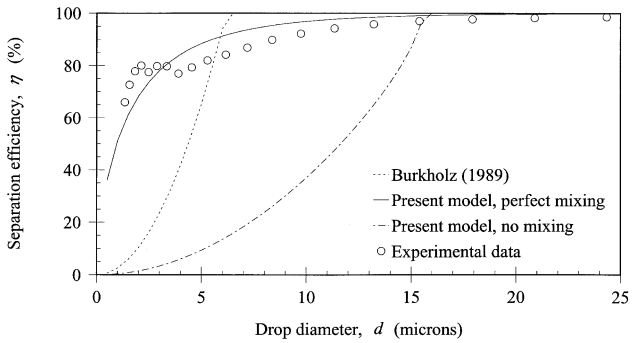

Figure 8. Separation efficiency vs. drop diameter.

Comparison between experimental measurements and the Bürkholz (1989) equation, and with models suggested in the present work. Cyclone type 3.A. Working conditions: air–water system, pressure 0.1 MPa, temperature 20°C, superficial gas velocity 5 m/s.

part, 1-A, contains the swirling element; the middle part, 2-A, contains the drainage system; and the upper part, 3-A, contains the outlet. The separation efficiency of the lower part was computed as the separation efficiency of a cyclone where the gas phase flows through an annulus. Because of the presence of the cone in the bottom part, the inner radius of the annulus has been assumed equal to half the radius of the cone (that is, $r_1 = 17.5$ mm and $r_2 = 55$ mm). The number of revolutions, $\bar{N}$, inside part 1-A is 0.5. The efficiencies of parts 2-A and 3-A, on the other hand, have been computed by considering that the gas phase flows through an empty tube with radius, r_2, equal to 55 mm and 27 mm, respectively; the number of revolutions is 1 in part 2-A and 0.3 in part 3-A.

The experimental data shown in Figure 8 refer to the axial flow separator type 3.A working with a superficial gas velocity of 5 m/s. The figure clearly shows that the present model, under the hypothesis of absence of mixing, is not able to predict the experimental data, whereas, both the present model, under the hypothesis of perfect radial mixing, and the equation suggested by Bürkholz (1989) seem to properly predict the trend of the experimental data. This result is particularly interesting because, contrary to the Bürkholz relation (1989), the present model does not introduce any adjustable parameters.

Figure 9 shows the comparison between three sets of experimental data obtained by testing the behavior of separator type 3.A, and values computed using the present model and the Bürkholz equation (1989). The figure shows that under the hypothesis of perfect radial mixing, the present model seems to predict the separation efficiency with acceptable accuracy for all of the working conditions analyzed.

Figure 10 shows the contribution of each zone of the separator toward the capture efficiency as predicted by the present model, under the hypothesis of perfect radial mixing. The results refer to separator 3.A working with a superficial gas-phase velocity of 15 m/s. For instance, the model predicts that drops of 6 μm are captured with an efficiency of about 65% in the lower zone, 1-A. Then, the efficiency increases up to 80% after the second part, and eventually reaches 95% at the end of the third zone, 3-A, that is, at the separator outlet.

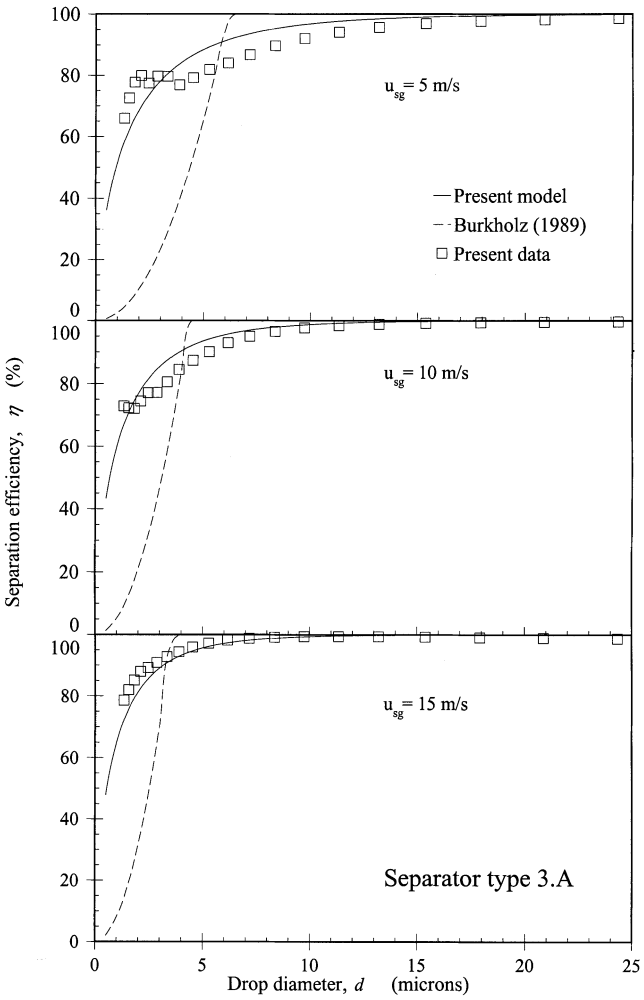

Figure 9. Separation efficiency vs. drop diameter.

Comparison between experimental measurements and the Bürkholz (1989) equation, and with the present model under perfect mixing hypothesis: cyclone type 3.A. Working conditions: air–water system, pressure 0.1 MPa, temperature 20°C, superficial gas velocity (A) 5 m/s, (B) 10 m/s, (C) 15 m/s.

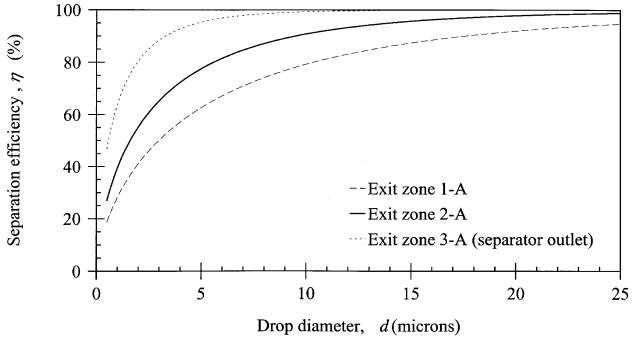

Figure 10. Separation efficiency vs. drop diameter, computed with the present model under perfect mixing hypothesis.

Contribution of each zone of cyclone type 3.A to separation efficiency. Working conditions: air–water system, pressure 0.1 MPa, temperature 20°C, superficial gas velocity 15 m/s.

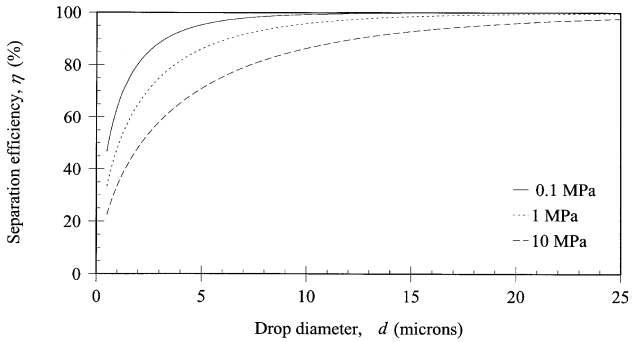

Figure 11. Separation efficiency vs. drop diameter, computed with the present model under perfect mixing hypothesis.

Effect of system pressure on separation efficiency of cyclone type 3.A. Working conditions: air–water system, temperature 20°C, F-factor 16 $Pa^{0.5}$.

The extension of the model to high pressures is shown in Figure 11, where separation efficiencies vs. drop diameter are shown for system pressures of 0.1, 1 and 10 MPa. An F-factor of 16 $Pa^{0.5}$ has been assumed, as suggested by experiments carried out at atmospheric pressure. The extension to high-pressure application has been made by assuming that the F-factors, and, hence, the shear stresses, have a constant value, as suggested by Perry and Green (1997). This assumption implies that, in relation to the properties of the fluids to be used, a higher mass flow rate and lower volumetric flow rate are permitted with an increase in pressure. The figure shows that for a given drop diameter, the efficiency decreases with an increase in pressure. This behavior is mainly due to two factors. First, the diminished difference in density between the liquid and the gas phases, which renders the separation more difficult. The other, and more important, factor is the lower permitted volumetric flow rate, which in turn means that a lower centrifugal force is imparted to the droplet when the system pressure increases. For example, the model predicts that a drop with a diameter of 6 μm is separated with an efficiency of 95% at 0.1 MPa, of 90% at 1 MPa, and 75% at 10 MPa.

Cyclone type 3.B was divided into four parts for computational reasons: 1-B, 2-B, 3-B, 4-B. Parts 1-B and 3-B were considered in the same way: as a gas phase flowing through an annulus, the inner radius is equal to the radius of the helix core (that is, 13.5 mm), whereas the outer radius is equal to $D/2$ (that is, 67.5 mm). In parts 2-B and 4-B the gas phase is also considered to be flowing through an annulus, but the outer radiuses are, respectively, the outside radius of the drainage chamber (96 mm) and the radius of the concentric tube (105 mm) used to limit the reentrainment phenomena. The number of revolutions inside the separator is 2.5 for zone 1-B, 1 for zone 2-B, 1.25 for zone 3-B, and 1.25 for zone 4-B.

Figure 12 shows the comparison between the present experimental data, obtained by testing the type 3.B separator, and the computed trends evaluated using the present model under the hypothesis of perfect radial mixing. The figure shows that even if the geometry of the swirling element is changed, the model seems to predict the separation efficiency properly.

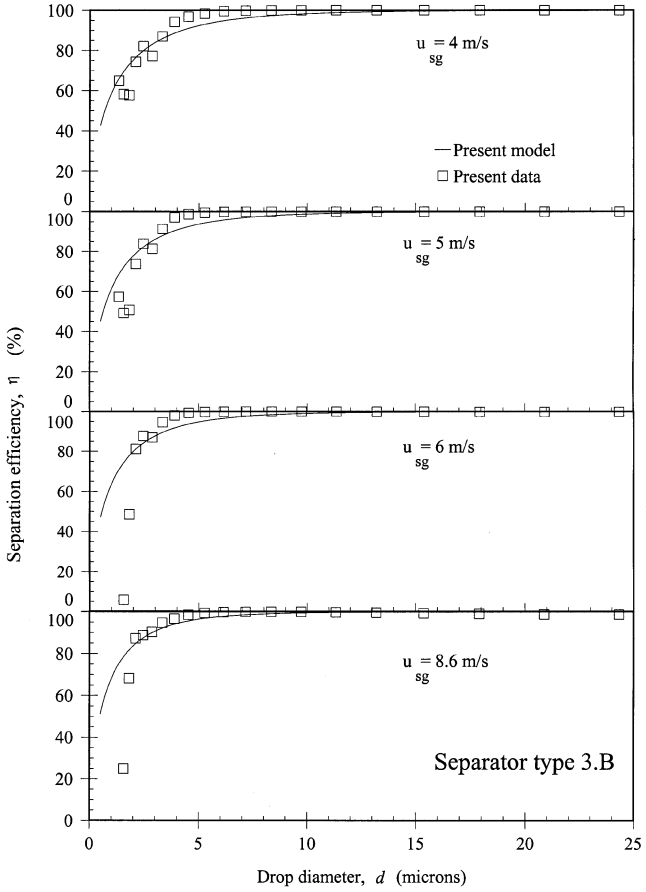

Figure 12. Separation efficiency vs. drop diameter.

Comparison between experimental measurements and the present model under perfect mixing hypothesis: cyclone type 3.B. Working conditions: air–water system, pressure 0.1 MPa, temperature 20°C, superficial gas velocity (A) 4 m/s, (B) 5 m/s, (C) 6 m/s, (D) 8.6 m/s.

Figure 13 shows the comparison between experimental data and the computed trends, evaluated using the present model under the hypothesis of perfect radial mixing, for the type 3.C cyclone. For computational reasons, cyclone type 3.C was divided into four parts, the same as the type 3.B cyclone. The only difference between the two cyclones is the presence of the cone in the type 3.C cyclone. Therefore, in the latter case, the flow of the gas phase through part 1-C has been considered to be the flow though an annulus of the inner radius equal to half the cone radius, that is, $r_1 = 32.5$ mm. Figure 13 shows that the present model tends systematically to underestimate the separation efficiency. This behavior is probably due to the simplifying hypothesis used to simulate the part 1-C. In fact, it has been assumed that the separation efficiency of the cone is equal to the separation efficiency of a cylinder, with the inner radius equal to half the cone radius. This assumption allows us to simplify the mathematical model but, as shown in figure, it introduces systematic errors.

The potentialities of the axial flow cyclone are evident from the analysis of the Figure 14, which shows a comparison between an axial flow cyclone and a wire-mesh mist eliminator. The example refers to a flow rate of 100,000 kg/h of air at 7 MPa and 20°C. In order to avoid reentrainment phenomena,

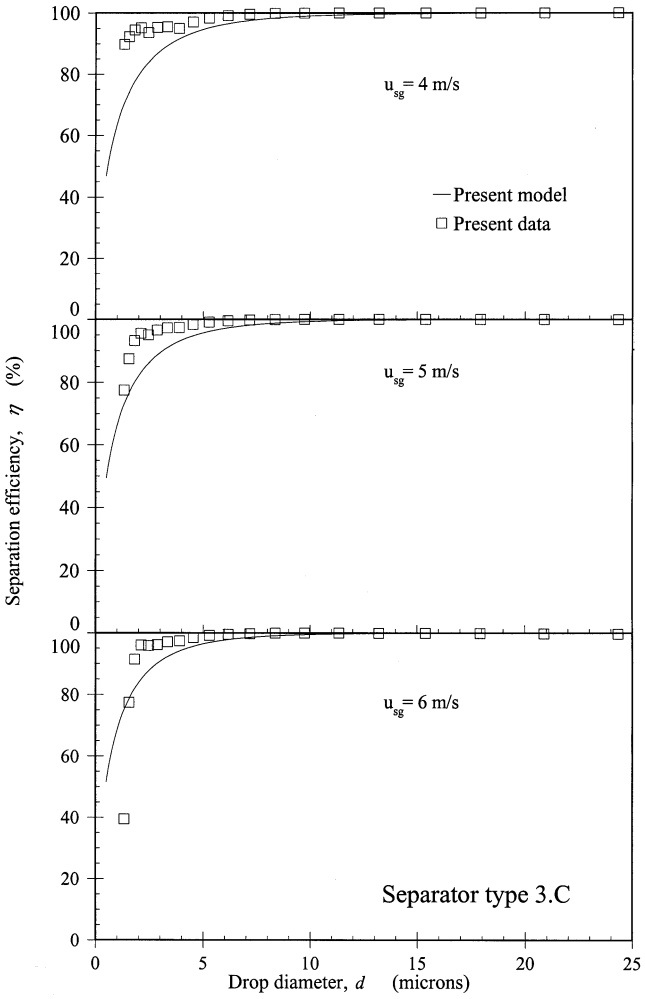

Figure 13. Separation efficiency vs. drop diameter.

Comparison between experimental measurements and the present model under perfect mixing hypothesis: cyclone type 3.C. Working conditions: air–water system, pressure 0.1 MPa, temperature 20°C, superficial gas velocity (A) 4 m/s, (B) 5 m/s, (C) 6 m/s.

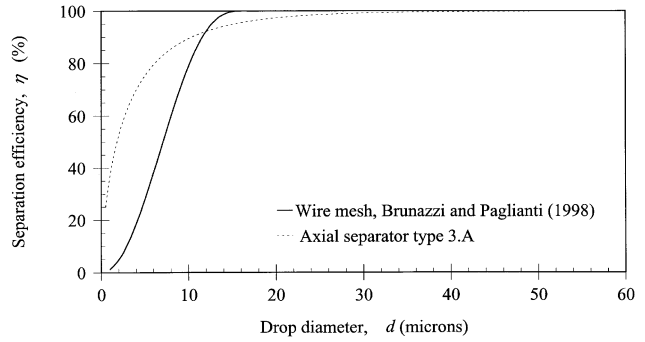

Figure 14. Separation efficiency vs. drop diameter, under high-pressure working conditions.

Comparison between theoretical behavior of wire-mesh mist eliminators (Brunazzi and Paglianti, 1998) and axial flow cyclones, present model. Wire-mesh packing characteristics: 270 m^2/m^3, wire diameter 270 microns, pad thickness 150 mm, superficial gas velocity 0.37 m/s. Cyclone characteristics: type 3.A, superficial gas velocity 1.7 m/s. Working conditions: air–water system, pressure 7 MPa, temperature 20°C.

the superficial gas velocity for wire-mesh mist eliminators has been assumed equal to 0.37 m/s, which corresponds to an F-factor of 3.37 $Pa^{0.5}$. Similarly, an F-factor equal to 16 $Pa^{0.5}$ has been assumed for the axial flow type 3.A cyclone, as explained previously. Figure 14 shows a comparison between the computed performances; the axial flow separator shows a higher separation efficiency for droplets smaller than 10 microns; whereas, somewhat higher efficiencies are shown by the wire-mesh mist eliminator above this limit up to about 30 microns, above which the efficiencies become comparable. Moreover, it is worth pointing out that when using a wire-mesh mist eliminator, a vessel with a 1070-mm internal diameter is necessary, whereas if a separator consisting of 21 axial-flow type 3.A cyclones arranged in parallel is used, the vessel diameter reduces to 900 mm. Finally, the use of axial-flow cyclones allows high separation efficiencies to be obtained across a broad range of droplet sizes, and also allows the vessel diameter to be sometwhat reduced, which is very important for high-pressure applications.

Conclusions

The experimental data on droplet removal efficiency presented in this article were obtained using a laser-based droplet sizer, the Malvern Particle Sizer. This article has presented not only different sets of separation efficiency of axial flow separators but also a new model for predicting their removal efficiency. Analysis of the experimental data obtained in this article shows that this new model can be used for predicting the separation efficiency of this new family of separators. The proposed model allows the measured efficiency to be predicted with sufficient accuracy without the need of introducing any adjustable parameters. This result is significant because no mechanistic model has yet been published in the literature to predict the separation efficiency of this family of separators. This could be an important improvement, as, especially for high working pressures, an increasing quantity of industrial separation equipment is now using axial-flow cyclones. In fact, axial-flow cyclones permit a reduction to be made in the diameter of the vessel containing the separator, thus, allowing an important reduction in investment costs. The new mechanistic model presented in this article could, therefore, be used for the design and the optimization of complex separation units.

Acknowledgments

This publication is based on work supported by Costacurta S.p.A. VICO, Via Grazioli 30, 20161 Milan, Italy and by the "Ministero dell'Università e della Ricerca Scientifica." The authors thank Ing. S. Sagripanti and Ing. A. Babbore for their helpful assistance, and Ing. B. Mondello and Ing. A. Luongo for some useful discussions.

Notation

C = constant of Eq. 2
C_D = drag coefficient
d = droplet diameter
dp_{100} = the smallest droplet diameter that can be separated with an efficiency equal to 100%
F-factor = $u_{sg} \cdot \sqrt{\rho_g}$
K = constant of Eq. 1
L = cyclone length
N = total number of droplets in the control volume

$\bar{N}$ = number of revolutions inside the separator
n = exponent of Eq. 2
r = radius
Q = gas volumetric flow rate
T = temperature
t = time
t_{res} = residence time
u = gas velocity
$\bar{u}_\theta$ = mean tangential gas velocity
u_{sg} = superficial gas velocity
X = droplet concentration
z = axial distance

Greek letters

η = capture efficiency
μ = viscosity
ν = droplet velocity
π = 3.14159...
θ = angle
ρ = density

Subscripts and superscripts

a = axial
g = gas phase
l = liquid phase
r = radial
θ = tangential

Literature Cited

Alexander, R. M., *Air Pollution Control Engineering*, Chap. 6, Dekker, New York (1980).

Babbore, A. "Fluidodinamica ed Efficienza in Separatori Assiali Centrifughi," (in Italian), MSc Thesis, Univ. of Pisa, Pisa, Italy (2000).

Brunazzi, E., and A. Paglianti, "Design of Wire Mesh Mist Eliminators," *AIChE J.*, **44**, 505 (1998).

Brunazzi, E., and A. Paglianti, "Design of Complex Wire Mesh Mist Eliminators," *AIChE J.*, **46**, 1131 (2000).

Bürkholz, A., *Droplet Separation*, VCH, Weinheim, Germany (1989).

Capps, R. W., "Properly Specify Wire-Mesh Mist Eliminators," *Chem. Eng. Prog.*, **90**, 49 (1994).

Carpenter, C. L., and D. F. Othmer, "Entrainment Removal by a Wire-Mesh Separator," *AIChE J.*, **1**, 549 (1955).

Dietz, P. W., "Collection Efficiency of Cyclone Separators," *AIChE J.*, **27**, 888 (1981).

Fabian, P., P. Hennessey, M. Neuman, and P. Van Dessel, "Demystifying the Selection of Mist Eliminators," *Chem. Eng.*, **100**, 106 (1993).

Flagan, R. C., and J. H. Seinfeld, *Fundamentals of Air Pollution Engineering*, Prentice Hall, Englewood Cliffs, NJ (1988).

Holmes, T. L., and G. K. Chen, "Design and Selection of Spray/Mist Elimination Equipment," *Chem. Eng.*, **91**, 82 (1984).

Licht, W., *Air Pollution Control Engineering*, Dekker, New York (1980).

Ludwig, E. E., *Applied Process Design for Chemical and Petrochemical Plants*, Vol. 1, 3rd ed., Chap. 4, Gulf Pub., Houston, TX (1995).

Perry, R. H., and D. W. Green, *Perry's Chemical Engineers' Handbook*, 7th ed., Chap. 26, McGraw-Hill, New York, p. 26 (1997).

Svrcek, W. Y., and W. D. Monnery, "Design Two-Phase Separators Within the Right Limits," *Chem. Eng. Prog.*, **89**, 53 (1993).

Verlaan, C. C. J., "Performance of Novel Mist Eliminators," PhD Thesis, Delft Univ., Delft, The Netherlands (1991).

York, O. H., and E. W. Poppele, "Wire Mesh Mist Eliminators," *Chem. Eng. Prog.*, **59**, 45 (1963).

Ziebold, S. A., "Demystifying Mist Eliminator Selection," *Chem. Eng.*, **107**, 94 (2000).

Manuscript received Manuscript received Feb. 15, 2001, and revision received May 28, 2002.